Integrated Photonic K_u-Band Beamformer Chip With Continuous Amplitude and Delay Control

Maurizio Burla, David Marpaung, Leimeng Zhuang, *Member, IEEE*, Arne Leinse, Marcel Hoekman, René Heideman, and Chris Roeloffzen, *Member, IEEE*

***Abstract*— We present the first demonstration of a broadband and continuously tunable integrated optical beamforming network (IOBFN) capable of providing continuously tunable true-time-delay up to 236 ps over the entire DVB-S band (10.7–12.75 GHz), realized with a CMOS compatible process. The tunable delays are based on reconfigurable optical ring resonators in conjunction with a single optical sideband filter integrated on the same optical chip. The delays and filter responses are software programmable. Four tunable delay lines are integrated on a single chip and configured to feed a 16-element linear antenna array. The broadband beam steering capability of the proposed IOBFN is demonstrated by the squint-free antenna pattern generated from the measured RF amplitude and phase responses of the optical delay line.**

***Index Terms*— Microwave photonics, optical beamforming, optical ring resonators, phased array antenna, photonic signal processing, true-time-delay.**

I. Introduction

In RECENT years, satellite communications (SATCOM) systems have been aiming towards higher operating frequencies in order to provide wider bandwidths for the ever-increasing need of data rate. Most of the currently deployed systems operate at K_u-band and are moving towards even higher frequencies (e.g. K_a-band). Phased array antennas are very useful in SATCOM applications, thanks to the capability to produce highly-directive beams which can be shaped and scanned electronically [1]. In general, however, for modern applications where large instantaneous bandwidths are required, true-time-delay (TTD) must be used in place of phase shift for the array control. To date, purely electronic solutions for TTD cannot meet the requirements [1], and a number of photonic solutions have been proposed [2]–[4] to overcome the limitations of electronic TTDs, namely low-frequency or narrowband operation, limited amount of delay, discontinuous tunability, and more. Nonetheless, photonic solutions are often regarded with certain skepticism due to the generally high bulk, low system performance and high costs [5]. In the current challenge towards providing the high performance typical of photonic solutions, while retaining the advantages offered by microelectronics (very low space occupation, consumption, and unit cost), several authors see in integrated microwave photonics (IMWP) an answer to this need, as an enabling technology for the exploitation and the large-scale deployment of the advantages of microwave photonics [5], [6]. In line with this approach, in [7] we have proposed an integrated, continuously tunable beamformer realized with a CMOS compatible process [8] which demonstrated operation over approx. 1 GHz in L-band (1–2 GHz) [7], while in [9] we proposed a single integrated K_u-band TTD line.

In this letter, for the first time, we demonstrate the performance of a complete microwave photonic integrated beamformer (IOBFN) which has been obtained by combining multiple of the individual TTD lines proposed in [9] to form a binary-tree beamformer, with continuously tunable amplitude and group delay responses. Compared to our previous demonstration in [7], the proposed IOBFN now brings together *all* the desired TTD characteristics, being capable of operating *directly* at high RF frequencies (K_u-band), without need of prior downconversion, continuously and seamlessly tunable, integrated in a chip realized with a CMOS-compatible process, thus very compact and potentially very low-cost for large production volumes. In addition to that, the instantaneous bandwidth has been doubled (2.05 GHz versus 1 GHz in [7]) We show its performance down to the application level by displaying that the generated antenna patterns exhibit a broadband performance over the complete band, without the undesired beam squint phenomenon [1], thus proving the effectiveness of the proposed IOBFN.

II. Principle

The implementation of TTD using filters based on optical ring resonators (ORR) was proposed by Rasras *et al.* [10] and demonstrated in several applications [7], [11]. The group delay T_{group} at $\omega_c + \omega_{\text{RF}}$ is defined as:

$$T_{\text{group}} = \left.\frac{\partial \varphi(\omega)}{\partial \omega}\right|_{\omega_c+\omega_{\text{RF}}} \tag{1}$$

Manuscript received February 1, 2013; revised March 14, 2013; accepted April 6, 2013. Date of publication April 12, 2013; date of current version May 30, 2013. This work was supported in part by Agentschap NL, Dutch Point One R&D Innovation Project Nr. PNE101008.

M. Burla was with the University of Twente, Enschede 7522 NH, The Netherlands. He is now with the Institut National de la Recherche Scientifique-EMT, Montréal H5A 1K6, Canada (e-mail: maurizio.burla@emt.inrs.ca).

D. Marpaung was with the University of Twente, Enschede 7522 NH, The Netherlands. He is now with the Centre for Ultrahigh Bandwidth Devices for Optical Systems, University of Sydney, Sydney 2006, Australia (e-mail: d.marpaung@physics.usyd.edu.au).

L. Zhuang is with the University of Twente, Enschede 7522 NH, The Netherlands (e-mail: l.zhuang@ewi.utwente.nl).

A. Leinse, M. Hoekman, and R. Heideman are with LioniX B.V., Enschede 7500 NH, The Netherlands (e-mail: a.leinse@lionixbv.nl; m.hoekman@lionixbv.nl; r.g.heideman@lionixbv.nl).

C. Roeloffzen is with the University of Twente, Enschede 7522 NH, The Netherlands, and also with Satrax B.V., University of Twente, Enschede 7522 NH, The Netherlands (e-mail: c.g.h.roeloffzen@utwente.nl).

Color versions of one or more of the figures in this letter are available online at http://ieeexplore.ieee.org.

Digital Object Identifier 10.1109/LPT.2013.2257723

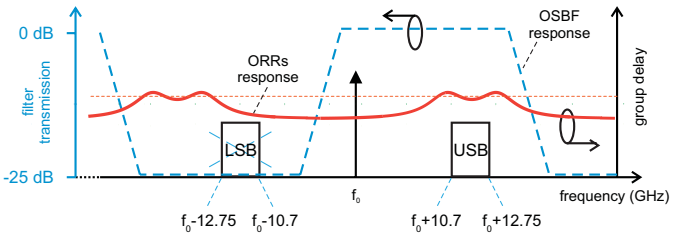

Fig. 1. Principle of operation of the optical true time delay lines based on ORRs and OSBF.

that is, the phase slope at the same frequency point. A linear phase response (i.e. a constant group delay, as desired) can be approximated by the 2π phase transition offered by an ORR around its resonance frequency, and the phase slope (i.e. group delay) can be tuned continuously by tuning the resonator response [7]. Multiple ORRs can be cascaded to increase the available delay bandwidth while keeping the delay ripple below the maximum desired value [12]. Since a tradeoff exists between the delay bandwidth and the amount of delay that can be generated with a maximum acceptable phase error, it is advantageous to employ optical single-sideband (OSSB) modulation in order to limit the bandwidth requirement of the desired linear phase characteristic over the span of one sideband only [13]. In this experiment we generate optical single-sideband full-carrier (OSSB-FC) modulation by employing an optical sideband filter (OSBF) to suppress one of the sidebands of an intensity-modulated (IM) optical carrier, while the carrier and the desired sideband lie within the filter passband (Fig. 1). In this way it is possible to configure the ORR responses to generate the correct delay over the upper sideband only (Fig. 1).

The RF phase shift provided to the information signal can be controlled either in the electrical domain, e.g. using a broadband RF phase shifter, or directly in the optical domain, e.g. using the separate carrier tuning principle as demonstrated in [11], [13].

III. Realization and Measurements

A. Chip Layout

The proposed IOBFN implements the ORR-based delay generation concept described above and has been realized in low-loss TriPleX^{TM} waveguide technology [8]. The schematic is shown in Fig. 2. The IOBFN features a binary-tree structure where ORRs have been placed in each branch in order to have independently tunable delay responses for each channel. In addition, any desired amplitude ratio among the 4 channels can be selected by programming the tunable couplers C1, C2 and C3 on the chip. When an individual I/O path is selected, the ORRs of that path are tuned to create the phase slope required for the desired delay, as in Eq. (1) [7]. On the same chip, an OSBF of the type "Mach-Zehnder interferometer (MZI) + ring" is shared among the channels to realize the OSSB-FC modulation, as previously discussed. In [7] the detailed layout of the microwave photonic chip has been described. Current implementations include up to 16 optical channels in a single chip [5].

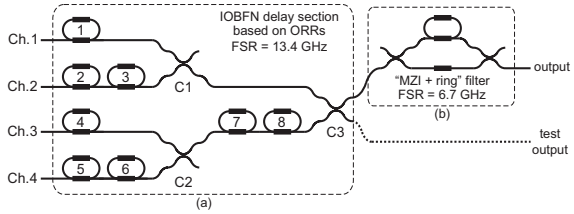

Fig. 2. Schematic of the IOBFN: (a) delay lines based on cascaded ORRs; (b) OSBF used for OSSB-FC modulation.

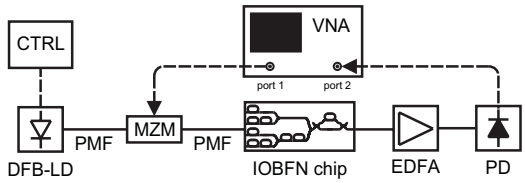

Fig. 3. Schematic of the measurement setup. CTRL: laser control electronics.

B. Measurement Setup

The measurement setup is shown in Fig. 3. An EM4 high-power laser produces a 100 mW optical carrier in the 1550 nm band, which is intensity modulated (IM) using an Avanex FA20 Mach-Zehnder modulator (MZM) biased in quadrature. The RF modulating signal is generated by an Agilent N5230A vector network analyzer (VNA). The IM signal is then fed to the optical chip, on which the OSBF is thermo-optically programmed to filter out the lower sideband and to implement the variable delay, as graphically shown in Fig. 1. An erbium-doped fiber amplifier (EDFA) is used to compensate for the fiber-to-chip coupling losses, which will be reduced in future implementations by integrating suitable spot-size converters. The amplified signal enters a Discovery Semiconductor DSC 710 high-power photodetector (PD). The RF output of the detector is connected to port 2 of the VNA for the amplitude and phase measurements.

C. OSBF Response

Fig. 4 shows the measured RF magnitude and group delay responses of the optical sideband filter overlapped to the IM signal to be processed. For this measurement, a 50 MHz modulating tone is produced by port 1 of the VNA and the optical carrier wavelength is swept over the band of interest (phase shift method [14]). The frequency response of the OSBF repeats periodically every FSR, which is approximately 6.7 GHz. By properly tuning the wavelength of the optical carrier, as shown in Fig. 4, it is possible to let the unwanted sideband fall in one of the stopbands of the OSBF, while the desired sideband passes undistorted through one of the pass-bands. The optical carrier is also passed through a passband (see Fig. 4, top). In this way the periodicity of the OSBF was employed to generate OSSB-FC over an RF signal in the DVB-S band (10.7–12.75 GHz) without need of prior RF downconversion.

From Fig. 4 it can be noticed that the suppression in the OSBF stopbands varies across frequency. This can be attributed to the group index change in the bends of the ring, which makes the optical path length of the ORR not exactly

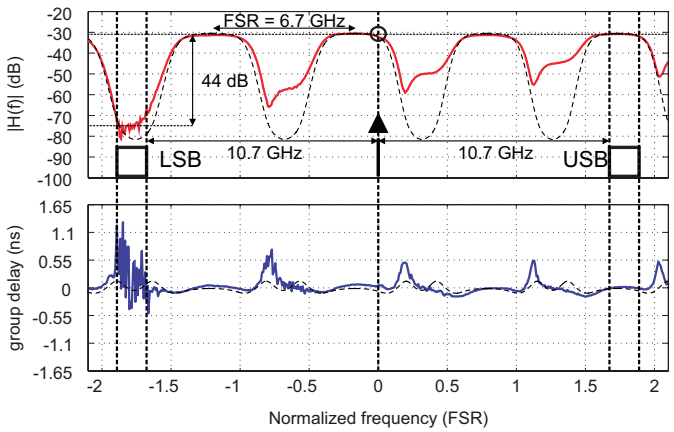

Fig. 4. Measured (solid) and simulated (dashed) magnitude (top) and group delay response (bottom) of the OSBF used to suppress the undesired sideband. Note the high flatness of the group delay characteristic over the passband.

twice the length difference between the arms of the MZI [15]. Nonetheless, the tunability of the filter allowed to reconfigure the response in such a way to obtain maximum suppression over the undesired stopband, that is, between 10.7 GHz and 12.75 GHz below the carrier frequency (Fig. 4, top), without any degradation of the passband flatness.

After the lower sideband is suppressed (Fig. 4), the ORRs in each channel of the IOBFN (Fig. 2a) can be tuned in such a way to achieve the desired delay (see [7] for more details on the delay tuning procedure).

D. RF Magnitude and Phase Responses

In order to point the beam of the antenna array to an arbitrary direction ϑ_0, the delay produced by the n-th IOBFN channel should be [1]

$$\tau_n = \frac{nd\sin(\vartheta_0)}{c_0} \tag{2}$$

where d is the inter-element distance and c_0 is the speed of light in vacuum. Let us assume to use the IOBFN to feed a 16-elements linear antenna array operating at K_u-band with $d = 11.8$ mm. We divide the array in 4 sub-arrays of 4 adjacent elements each. Electronic TTDs based on MMIC technology [16] can be used to provide the smaller delay differences within each subarray [5], without impairing the overall broadband performance, while the IOBFN can provide the larger delay required among the subarrays, as shown in Fig. 5. An array of 4 external intensity modulators can be used for the connection to the IOBFN. In this configuration, from Eq. (2), in order to have $\vartheta_0 = 30°$ the delays of channels 1 through 4 should be 0 ps, 78.68 ps, 157.36 ps and 236.04 ps, respectively. Fig. 6 shows the measured RF magnitude and phase responses of the four channels, in the 10.7–12.75 GHz band, for the $\vartheta_0 = 30°$ delay setting. A group delay resolution is in the sub-ps range can be achieved, limited only by the employed control electronics [7].

The measured phase characteristics show good matching with their theoretical linear responses. The amplitude ripple in the band is below 3 dB, and can be attributed to a non-perfectly flat response of the OSBF and ORRs passbands.

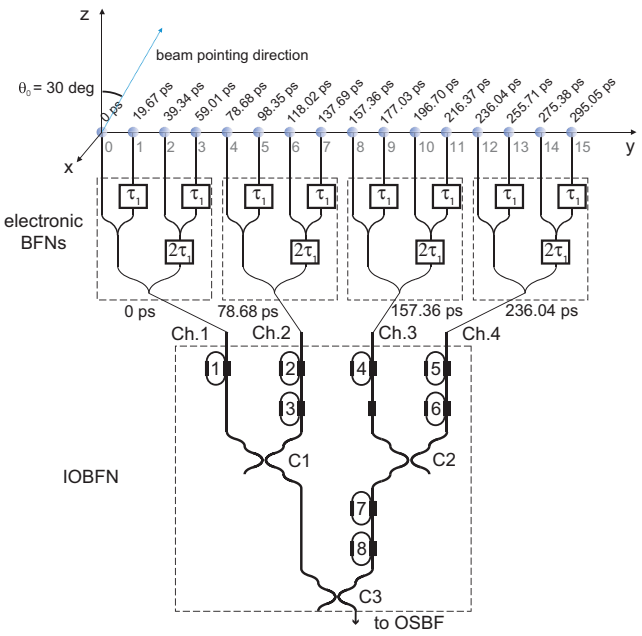

Fig. 5. Schematic showing the connection of the IOBFN to a 16-element antenna array. The delays required for each antenna element, calculated from (2), are also shown.

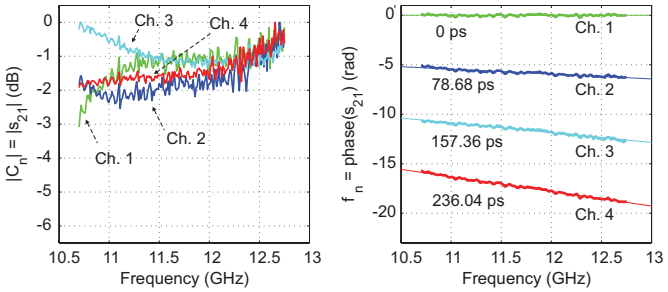

Fig. 6. Measured magnitude (left) and phase (right) responses at K_u band of the IOBFN channels. The displayed magnitude responses have been equalized using the tunable couplers C1-C3, and the effect of the fiber-to-chip loss ($\approx$ 6 dB/facet; lowered to 1.5 dB/facet in current implementations [8]) and the coupling loss in the couplers were removed.

The channels' attenuations increase when increasing the delay ($\approx$ 0.003 dB/ps) [8], as expected due to the longer propagation time in the waveguide, giving channel 4 (with highest delay) the highest additional loss ($\approx$ 0.7 dB). Equalization is achieved by balancing the channel powers via the tunable couplers C1 and C2, followed by C3 (Fig. 2). Thus, in all cases, the additional equalization loss keeps below 0.7 dB.

IV. Wideband Beamforming Demonstration

We can now evaluate the broadband IOBFN performance by analyzing the effect that the optically-generated TTDs have on the radiation pattern of the array, i.e. on the shape of the array factor (AF) and on the pointing direction of the main radiation lobe. Fig. 7(a) shows the simulated array factor versus pointing angle ϑ and frequency f, calculated from the measured magnitudes (C_n) and phases (φ_n) in Fig. 6, as [1]

$$F(\vartheta, f) = \sum_{n=0}^{N} C_n e^{j\varphi n} e^{jn\frac{2\pi f}{c_0}d\cos\vartheta} \tag{3}$$

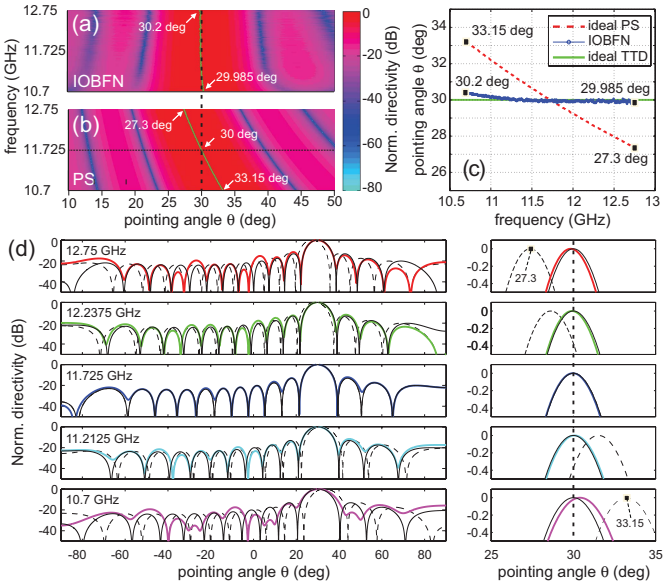

Fig. 7. Simulated array factor versus angle and frequency (a) for the IOBFN and (b) for the case of phase shifters. (c) Pointing direction comparison. (d) Comparison at different frequencies: phase shift (dashed), ideal TTD (solid, thin), and proposed OBFN (solid, thick). Right: zoom around $\vartheta = 30°$.

Fig. 7(a) shows that the direction of the main lobe (green line) does not vary sensibly across frequency, keeping in close proximity of the desired $\vartheta_0 = 30°$ value. Fig. 7(d) shows the same array factor (thick solid lines) at five equally-spaced frequencies within the DVB-S band (10.7, 11.2125, 11.725, 12.2375 and 12.75 GHz). We can observe that the calculated AF (thick solid lines) follows closely the shape of the one that would be obtained when ideal TTDs are used (thin solid lines). A zoom around ϑ_0 shows that the error in the pointing direction is very low, in the order of a hundredth of a degree (0.02° at 11.2125 GHz, 0.04° at 11.725 GHz, 0.015° at 12.2375 GHz and 12.75 GHz), which corresponds to the 0.034% of the total beamsteering angle (30°). At 10.7 GHz, the error rises to 0.2°, which is still as low as the 0.67%. If we assume that adjacent geosynchronous satellites are spaced approximately 2°, the measured error is negligible for SATCOM applications.

It is important to compare this result with the common case of phase-shifters (PS) based beamforming, where the phase excitations of each element would be constant in frequency. Assuming the phase shift is calculated to generate a beam with 30° pointing direction at mid-band (11.725 GHz), the corresponding array factor would be as shown in Fig. 7(b). It is clearly visible that the use of PS instead of the proposed IOBFN would create a strong variation of the pointing direction across the frequency band (beam squint). This can be seen even more clearly in Fig. 7(d), where the AF generated by PS is shown with dashed lines, and in Fig. 7(c), where the pointing direction versus frequency is plotted in the cases of using PS, ideal TTDs, and the IOBFN. The absolute errors are 2.7° at 12.75 GHz and 3.15° at 10.7 GHz, two orders of magnitude larger than those obtained with the proposed true-time-delay IOBFN, and unacceptable for SATCOM applications. This result demonstrates the need of employing TTD in broadband systems and the effectiveness of the proposed IOBFN to solve the squint problem for K_u-band phased array antenna beamsteering.

V. Conclusion

In conclusion, we have experimentally demonstrated, for the first time, broadband and continuously tunable true-time-delay beamforming using a compact integrated optical processor, over the complete DVB-S satellite communication band (10.7–12.75 GHz). The optical chip is realized in low-loss CMOS compatible waveguide technology and is capable of processing RF signals directly at K_u band, without need for prior down-conversion, exploiting the reconfigurability of the ORRs and the periodicity of the employed OSBF. These characteristics could be further exploited for processing even higher frequencies (e.g. K_a-band) or multiple bands simultaneously, e.g. in multi-wavelength optical signal processors [2] or incoherent microwave photonic filters (MPF) [3].

References

[1] R. J. Mailloux, *Phased Array Antenna Handbook*. Norwood, MA, USA: Artech House, 2005.
[2] N. A. Riza, *Selected Papers on Photonic Control Systems for Phased Array Antennas*. Bellingham, WA, USA: SPIE, Jun. 1997.
[3] J. Capmany, J. Mora, I. Gasulla, J. Sancho, J. Lloret, and S. Sales, "Microwave photonic signal processing," *J. Lightw. Technol.*, vol. 31, no. 4, pp. 571–586, Feb. 15, 2013.
[4] X. Yi, L. Li, T. Huang, and R. Minasian, "Programmable multiple true-time-delay elements based on a Fourier-domain optical processor," *Opt. Lett.*, vol. 37, no. 4, pp. 608–610, Feb. 2012.
[5] D. Marpaung, C. Roeloffzen, R. Heideman, A. Leinse, S. Sales, and J. Capmany, "Integrated microwave photonics," *Laser Photon. Rev.*, vol. 21, no. 7, pp. 1–33, Apr. 2013.
[6] R. Won, "Microwave Photonic Shines," *Nature Photon.*, vol. 5, no. 12, pp. 735–736, Dec. 2011.
[7] L. Zhuang, *et al.*, "Novel ring resonator-based integrated photonic beamformer for broadband phased array receive antennas—Part II: Experimental prototype," *J. Lightw. Technol.*, vol. 28, no. 1, pp. 19–31, Jan. 1, 2010.
[8] L. Zhuang, D. Marpaung, M. Burla, W. Beeker, A. Leinse, and C. Roeloffzen, "Low-loss, high-index-contrast Si_3N_4 SiO_2 optical waveguides for optical delay lines in microwave photonics signal processing," *Opt. Express*, vol. 19, no. 23, pp. 23162–23170, Nov. 2011.
[9] M. Burla, *et al.*, "CMOS-compatible integrated optical delay line for broadband Ku-band satellite communications," in *Proc. IEEE Int. Topical Meeting Microw. Photon.*, Sep. 2012, pp. 1–4.
[10] M. S. Rasras, *et al.*, "Integrated resonance-enhanced variable optical delay lines," *IEEE Photon. Technol. Lett.*, vol. 17, no. 4, pp. 834–836, Apr. 2005.
[11] M. Burla, *et al.*, "On-chip CMOS compatible reconfigurable optical delay line with separate carrier tuning for microwave photonic signal processing," *Opt. Express*, vol. 19, no. 22, pp. 21475–21484, Oct. 2011.
[12] M. Burla, C. G. H. Roeloffzen, D. A. I. Marpaung, M. R. H. Khan, and W. C. van Etten, "A novel design procedure for minimum RF phase error in optical ring resonator-based integrated optical beamformers for phased array antennas," in *Proc. IEEE Photon. Benelux Chapter*, Nov. 2010, pp. 245–248.
[13] S. Chin, *et al.*, "Broadband true time delay for microwave signal processing, using slow light based on stimulated Brillouin scattering in optical fibers," *Opt. Express*, vol. 18 no. 21, pp. 22599–22613, Oct. 2010.
[14] K. Daikoku and A. Sugimura, "Direct measurement of wavelength dispersion in optical fibres-difference method," *Electron. Lett.*, vol. 4, no. 5, pp. 149–151, Mar. 1978.
[15] C. G. H. Roeloffzen, "Passband flattened binary tree structured add-drop multiplexers using SiON waveguide technology," Ph.D. dissertation, Dept. Electr. Eng., Math. Comput. Sci., Univ. Twente, Enschede, The Netherlands, 2002.
[16] H. Hashemi, *et al.*, "Integrated true-time-delay-based ultra-wideband array processing," *IEEE Commun. Mag.*, vol. 46, no. 9, pp. 162–172, Sep. 2008.